Results in Engineering 24 (2024) 102872

Contents lists available at ScienceDirect

Results in Engineering

journal homepage: www.sciencedirect.com/journal/results-in-engineering

Research paper

Channel flow dynamics of fractional viscoelastic nanofluids in molybdenum disulphide grease: A case study

Maria Javaid [a,b,*], Junaid N. Chauhdary [a,c], M. Yasar Javaid [d], Muhammad Farooq [e,**], Faisal Saleem [f], M. Imran [b], Ijaz Hussain [g], M. Sultan [h], M. Imran Khan [e], Mohammad Ilyas Khan [i], Mohammad Rehan [j], Fahid Riaz [k,**]

[a] Research Center of Fluid Machinery Engineering and Technology, Jiangsu University, Zhenjiang, 212013, China
[b] Department of Mathematics, Government College University Faisalabad, Faisalabad, 38000, Pakistan
[c] Water Management Research Centre, University of Agriculture Faisalabad, Faisalabad, 38000, Pakistan
[d] Department of Mechanical Engineering Technology, Government College University Faisalabad, Faisalabad, 38000, Pakistan
[e] Department of Mechanical Engineering, College of Engineering, Prince Mohammad Bin Fahd University, Al-Khobar, Saudi Arabia
[f] Department of Chemical and Polymer Engineering, UET Lahore, Faisalabad campus, Pakistan
[g] Interdisciplinary Research Center for Refining and Advanced Chemicals, King Fahd University of Petroleum and Minerals, Dhahran 31261, Saudi Arabia
[h] Department of Agricultural Engineering, Bahauddin Zakariya University, Multan 60800, Pakistan
[i] Department of Chemical Engineering, College of Engineering, King Khalid University, Abha, Saudi Arabia
[j] Center of Excellence in Environmental Studies (CEES), King Abdulaziz University, Jeddah, Saudi Arabia
[k] Department of Mechanical Engineering, Abu Dhabi University, Abu Dhabi, United Arab Emirates

ARTICLE INFO

Keywords:
Fractional viscoelastic nanofluid
Heat and mass transfer
Molybdenum disulphide
Grease

ABSTRACT

Nanoscopic fluids especially viscoelastic Nanofluids are very useful in engineering and industrial problems. This research is to determine the open channel flow of a viscoelastic nanofluid (namely Oldroyd-B (OBNF)). Oldroyd-B fluid (OBF) was used as the base fluid and molybdenum disulphide nanopatrials were added in the fluid to form desired OBNF. To convert the mathematical model to a fractional model from a classical order partial differential equation PDE, fractional type derivative named Caputo-Fabrizio (CF) was used. The main objective of this study is to find the exact mathematical solution for the temperature, concentration and velocity distributions by using integral transformation technique. Final results are discussed graphically for the influence of different parameters on calculated temperature, concentration and velocity. Skin friction of the said fluid and engineering related dimensionless numbers including Reynolds number (Re), Prandtl number (Pr), Grashof number (Gr) and Schmidt number (Sc) are also discussed. At the end a comparison is illustrated in graphical form between current studied fluid (i.e. OBNF), another non-Newtonian fluid (i.e. Maxwell Nanofluid (MWNF)) and Newtonian fluid. As we know speed of Newtonian fluid is greater than non-Newtonian fluid, the same statement is validated by our solution. It is also noted that adding molybdenum disulphide nanoparticles to grease, heat transmission increased to 19.11% and mass transmission decreased to 2.51%.

1. Introduction

In present era, heat transfer applications are very vast almost in every field of science. Nanofluid got more attention because of their ability to enhance capacity of heat transformation. Choi and Eastman [1] introduced nanofluid in late nineteenth century. Koriko et al. investigated MHD thixotropic nanofluid for bioconvection flow and use Optimal Homotopy Analysis Method for solving governing equations and find out that in cases of nanoparticles active control, by reducing the velocity and temperature, thermophoretic parameters were increased [2]. Rehman et al. discussed an exponentially stretched surface for three-dimensional flow and developed a model for MHD water-based nanofluid in which consider three types of nanoparticles. They concluded that Skin-friction is greater for CuO-water nanofluid and lesser for AL_2O_3–water nanofluid, and local Nusselt number came out greater for CuO-water nanofluid whereas lesser for Fe_3O_4-water nanofluid [3].

* Corresponding author at: Research Center of Fluid Machinery Engineering and Technology, Jiangsu University, Zhenjiang, 212013, China.
** Corresponding authors.
E-mail addresses: mariajavaid@gcuf.edu.pk (M. Javaid), mfarooq@pmu.edu.sa (M. Farooq), fahid.riaz@adu.ac.ae (F. Riaz).

https://doi.org/10.1016/j.rineng.2024.102872
Received 13 July 2024; Received in revised form 26 August 2024; Accepted 8 September 2024
Available online 18 September 2024

Nomenclature

ρ	Density	μ	Dynamic viscosity
c_p	Heat capacity at constant pressure	α	Fractional parameter
k	Thermal conductivity	ν	Kinematic viscosity
T_w	Temperature	s	Laplace transform parameter
T_∞	ambient Temperature	n	Fourier transform parameter
C_w	concentration	s	Laplace transform parameter
C_∞	ambient concentration	Re	Reynolds number
$\mathbf{v}$	Velocity	Pr	Prandtl number
g	Gravity force	Gr	Grashof number
λ	Relaxation parameter	Sc	Schmidt number
λ_r	Retardation parameter		

Sheikholeslami studied Lorentz forces impact on Fe_3O_4 water, and concluded that heat transfer is increased by increase in radiation parameter and decreased by decrease in Lorentz forces [4]. Chamkha et al. used Keller box method and discussed the Nanofluid over an isothermal vertical wedge in a porous and thermal medium [5]. Wang et al. discussed minimum quantity lubrication of Nanofluid with a unique mechanism, process and device [6]. Liu et al. worked on magnetized stretched sheet and examined the flow of boundary-driven Maxwell nanofluid by using shooting scheme [7]. Bhattia et al. worked on a stretchable elastic surface and examined the flow of non-Darcian nanofluid flow, by used Keller-box numerical approach [8]. Dinarvand et al. studied thermomicropolar binary nanofluid numerically by using the bvp4c pattern of Matlab [9]. Basit et al. discussed two dimensional Sutterby nanofluid flow along a parabolic medium they also used bvp4c numerical method on Matlab [10]. Hasan et al. worked on 2-dimensional lid-driven cavity to investigate its flow pattern and thermal behavior. They concluded that the drag force and velocity field are greater at high Richardson numbers [11]. Hossain et al. worked on Magnetohydrodynamic (MHD) unsteady mixed convection for kerosene oil-based CNT nanofluid and concluded that increase in radiation intensity and dimensionless time improves fluid velocity, pressure, and temperature gradient but decreases the heat transfer rate of the semicircular heater [12]. Islam et al. studied water-based CNT-nanofluid and examined natural convection phenomena and find out that the heat transfer rate displays varied patterns varying the Rayleigh number, and it rises as the oscillation period increases. The fluid temperature and flow fields exhibit periodic behavior due to the sinusoidal heat source [13]. Azad et al. worked on MHD mixed convection in cylindrical coordinates they find out that the fluid flow and thermal performance boost up while the rotating speed of the cylinder is higher [14]. Hossain et al. studied numerically the time-dependent effect of low Reynolds number on Kerosene oil-based CNT nanofluid with magnetic field and radiation, their findings will be useful for designing thermal devices related to heat transfer, especially using the Kerosene oil-based CNT nanofluid under different conditions [15]. Hossain et al. worked in a magnetic field, used Oil-based nanofluids along with thermophysical properties to observe radiative domain. They use Galerkin residual technique based on finite elements methods [16]. Hasan et al. investigated the Rayleigh number and particle concentration effects in transient cavity flow by using Galerkin residual method and concluded that when the nanoparticle concentration rises, the heat transfer rate and average fluid temperature also increase [17]. Azad et al. worked numerically on nanofluid and study the effect of Hartmann number on combined convective flow in a horizontal channel. They concluded that physical parameters strongly affect the flow phenomenon and temperature field inside the cavity, whereas in the channel these effects are less significant [18].

In classical mathematics, fractional calculus is an important field. In which fractional order integral and differential operations are studied. In a conversation between L. Hopital and Leibniz via a letter about this content, in which they discussed how we can justify $\frac{\partial^m f}{\partial^m z}$ when $m = 1/2$? Leibniz suggested in his letter that there is a close relationship between derivatives and infinite divergent series, and $\frac{1}{\partial^2 z} = z\sqrt{\frac{dz}{z}}$. After their discussion many Famous mathematicians started working in this research area. In recent era the topic of this research has been expanded in different fields in different ways and scientist are working on this line, many researchers are working on it.

Shah et al. considered blood as base fluid along with gold nanoparticles and worked in an incline surface to study magnetohydrodynamic Casson nanofluid they found that increasing the volume percentage of gold nanoparticles from (0-0.04) percent gave an increase of up to 3.825% in the heat transfer rate [19]. Murtaza et al. worked on fractal fractional Casson nanofluid flow by using numerical methods and concluded that in response to 0.04 volume fraction of cadmium telluride nanoparticles, the rate of heat transfer increased by 15.27% and rate of mass transfer decrease by 2.07% [20]. Ahmad et al. used the fractal fractional differential operator and, as a coupled system of ODEs, expressed the feelings of love between Romeo and Juliet [21]. A well-known fractional differential operator is the Riemann-Liouville Fractional Differential Operator [22],

$$D_t^{\rho} g(t) = \begin{cases} \frac{1}{\Gamma(1-\rho)} \frac{d}{dt} \int_0^t \frac{g(\tau)}{(t-\tau)^{\rho}} d\tau, & 0 \le \eta < 1; \\ \frac{d}{dt} g(t), & \rho = 1, \end{cases} \tag{1}$$

where $\Gamma(\cdot)$ is known as Gamma function.

In recent era fractional calculus is advantageous in bioengineering [23] and biorheology [24]. “These derivatives are in fact improved differential equations, where integral time derivative has been replaced by fractional number” [25,26]. Recently many researchers work on fractionalized fluids and obtained the solutions. Abbas et al. studied brinkman fluid flow by using Prabhakar fractional derivatives, for mathematical calculations they use integral transformations and some numerical algorithms [27]. Siddique et al. worked on Jeffrey fluid and study magnetohydrodynamics and heat absorption effect on it by using the Prabhakar-like fractional derivative and concluded by some compressions that fractional model is better suited for describing the memory effect of the thermal and momentum fields [28]. Fetecau et al. discussed MHD unidirectional fractional Maxwell fluids, for fractional type model they used Caputo fractional derivative and calculate the fluid velocity, shear stress, and Darcy’s resistance graphically [29]. Rehman et al. used different fractional derivative operators and studied the second grade fluid flow in fractional form, like (i) Caputo hybrid derivative, (ii) Atangana Baleanu in Caputo sense, (iii) Caputo Fabrizio fractional derivative operators [30]. Beddrich et al. worked on time-fractional Navier–Stokes–Fokker–Planck system and introduced a new approach for numerical approximation [31].

Lubricants are actually the substances which are used on a machine’s parts to work smoothly. They used in oil as friction reducing agent between mechanical parts which are in contact with each other. These oils are used in motorized vehicles, where specifically they known as motor oils and transmission fluids. The use of lubricants in vehicles is essential to work vehicles properly. If the engine of a vehicle is lubricated properly, it needs less energy to move. So that vehicle consumes less fuel and long runs at low temperature. Similarly use of lubricant in other machinery is also essential to improve its efficiency. Actually lubricant play some basic roles in a machine first of all it reduces the friction which improve engine efficiency and reduce fuel consumption, keep engine clean, improving seal tightness, improve the service life of the engine and cooling the engine. Sometimes water is also used as lubricant in industrial area. Grease is commonly used lubricant which is actually a thick oily substance. Lubricating greases are typically combination of three ingredients: (i) oil, (ii) thickener, (iii) additives, which keep them in a semi-solid state. It is actually the combination of Thickener (5%-20%), Base oil (80%-95%), Additives (0%-10%). Thickeners reduce the friction between moving objects, additives enhance the ability of lubricating of the base oil, and also improve the ability of object to protect against wear and rust. It used to reduce the friction in machinery. Different types of greases are available in the market e.g. aluminum, lithium, Dielectric, synthetic and mineral based etc. Molybdenum Disulphide Grease is a multi-purpose grease, based on mineral base oils, lithium thickener and molybdenum disulphide, it forms a chemical reaction with metal surfaces which reduces friction which is known as boundary lubrication. It s mostly used for the lubrication of earthmoving equipments, agricultural machinery, homokinetic joints and heavy loaded plain bearing. Paszkowski [32] worked on mineral oil (ORLEN OIL SN-400) based lubricating greases, where lithium 12-hydroxystearate used as thickener and studied thixotropy. Through experimental work he finds a mathematical relation for lithium grease, which have wide application in lubrication system. Saeed and Kim studied nanofluid as a coolant in mini-channel heatsinks [33]. Yiling et al. worked on zirconium phosphate intercalated along with the thickener octadecyltrimethylammonium bromide (STAB-ZrP). Recently, Fabian et al. studied the prototype formulations and characterization with the help of LTS behavior, outgassing, and tribological performance [34]. Paszkowski et al. studied thixotropy of lithium lubricating greases [35]. Zhou et al. with the help of a fibrous structure worked on shear degradation of lubricating greases [36]. Fan et al. discussed Tribological properties of conductive lubricating greases [37].

Inspired by the above literature review and to close the loopholes, the objectives of the current work have been designed (1) to study non-Newtonian Nanofluid by considering an open channel flow of Oldroyd-B Nanofluid (OBNF) along with heat and mass transfer, placed between two parallel walls through integral transform technique for exact solution. (2) Furthermore, dimensionless numbers including Re, Pr, Gr and skin friction were calculated and a comparison was performed between Newtonian and non-Newtonian fluids. Previous researchers worked on Newtonian fluid or on simplest non-Newtonian fluids. In this work more complex type of viscoelastic non-Newtonian fluid is used whose mathematical study will be much useful as compare those fluids.

2. Methodology

Fractional differential operator is used for convert an ordinary type fluid to a fraction type model. Which is much useful as compare to ordinary differential model. Atangana in his book "Fractal-fractional differentiation and integration: connecting fractal calculus and fractional calculus to predict complex system" define different differential operators in detail [38]. In this research Caputo- Fabrizio Time-fractional Differential Operator is used which is defined as [39,40],

$$ {}^{CF}D_{\mathfrak{T}}^{\alpha} f(t) = \frac{M(\alpha)}{1-\alpha}\int_0^1 \exp\left[-\frac{\alpha(1-\mathfrak{T})}{1-\alpha}\right]\mathrm{F}(t)d\mathfrak{T}, \tag{2}$$

here, $M(\alpha)$ known as normalization function

$$M(0) = M(1) = 1.$$

There are three methods for solving differential equation analytically. One of the most popular method is integral transformation. In the book "Integral Transforms and their Applications", Debnath and Bhatta define different integral transformation [41].

The Laplace transform of $g(t)$ in $0 < t < \infty$ is,

$$G(s) = \mathcal{L}\{g(t)\} = \bar{g}(s) = \int_0^\infty e^{-st} g(t)dt; \quad \mathrm{Re}\, s > 0, \tag{3}$$

where, e^{-st} is kernel of the transform and s is transformed variable.

The inverse Laplace of Eq. (3) is

$$\mathcal{L}^{-1}\{G(s)\} = g(t) = \frac{1}{2\pi i}\int_{c-i\infty}^{c+i\infty} e^{st} G(s)\, ds; \quad c > 0. \tag{4}$$

Laplace transformation of Caputo Fabrizio (CF) time fractional derivative [38]

$$L\left[{}^{CF}D_{\mathfrak{T}}^{\alpha} f(t)\right] = \frac{saF(s)}{s + a_1},$$

where,

$$a = \frac{1}{1-\alpha}, a_1 = \frac{\alpha}{1-\alpha}.$$

The Fourier transform of $g(x)$ is defined as,

$$G(\kappa) = F\{g(x)\} = g_f(\kappa) = \int_{-\infty}^{\infty} e^{2\pi i\kappa x} g(\kappa)d\kappa, \tag{5}$$

where, κ is transformed variable. The inverse Fourier transformation of Eq. (5) is defined as

$$F^{-1}\{G(\kappa)\} = g(x) = \int_{-\infty}^{\infty} e^{2\pi i\kappa x} G(\kappa)d\kappa. \tag{6}$$

Fourier transformation is further classified into many types. The Fourier sine transform is one of them and defined as;

$$G(\kappa) = F\{G(x)\} = g_{fs}(\kappa) = \int_{-\infty}^{\infty} \sin(2\pi\kappa x) g(\kappa)d\kappa. \tag{7}$$

The inverse Fourier transformation of Eq. (7) is defined as

$$F^{-1}\{G(\kappa)\} = g(x) = \int_{-\infty}^{\infty} \sin(2\pi\kappa x) G(x)d\kappa. \tag{8}$$

2.1. Governing equations

Let us consider a flow of Oldroyd-B Nanofluid between two parallel plates placed vertically and septated by the distance k. For the improvement in heat transfer, MoS_2 are suspended uniformly in the base fluid. Consider the fluid motion is along x axes in the presence of buoyancy forces see Fig. 1. Initially both plates and the fluid everything is at rest with ambient temperature and constant concentration T_∞ and C_∞ respectively. After time $t > 0^+$, the temperature and concentration of the left plate increased to T_w and C_w. According to the conditions of the flow the velocity field, temperature and contraction are as follows,

$$\overrightarrow{V} = v_*(y,t), \tag{9}$$

$$T = T_*(y,t), \tag{10}$$

$$C = C_*(y,t). \tag{11}$$

Since, from literature history constitutive equations for continuity, momentum, temperature and contraction [42,43],

$$\nabla.\overrightarrow{V} = 0, \tag{12}$$

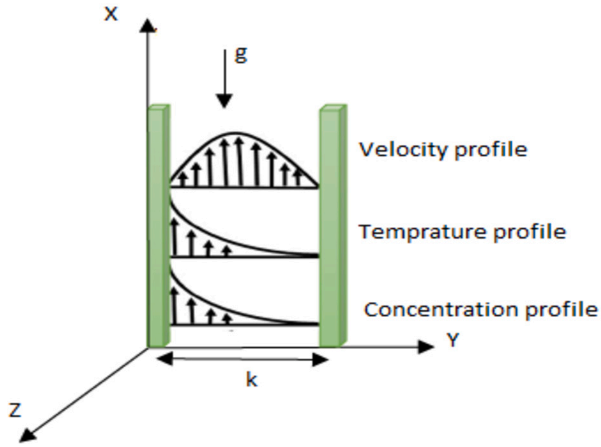

Fig. 1. Physical significance of the fluid flow

$$\frac{\partial V}{\partial t} = \frac{1}{\rho} div T + \vec{b}, \tag{13}$$

$$\frac{\partial T}{\partial t} = \frac{1}{\rho c_p}(k\nabla \times \nabla \times T), \tag{14}$$

$$\frac{\partial C}{\partial t} = D\nabla \times \nabla \times C. \tag{15}$$

According to the current discussed problem above equations are reduced to the form below,

$$\rho\left(1+\lambda_*\right)\frac{\partial v_*}{\partial t} = \mu\left(1+\lambda_{*r}\frac{\partial}{\partial t}\right)\frac{\partial^2 v_*}{\partial y^2} + \left(1+\lambda_*\frac{\partial}{\partial t}\right)(\rho\beta_T)g(T_*(y,t)-T_{*\infty}) + \left(1+\lambda_*\frac{\partial}{\partial t}\right)(\rho\beta_C)g(C_*(y,t)-C_{*\infty}), \tag{16}$$

$$\left(\rho C_P\right)\frac{\partial T_*}{\partial t} = k\frac{\partial^2 T_*}{\partial y^2}, \tag{17}$$

$$\frac{\partial C_*}{\partial t} = D\frac{\partial^2 C_*}{\partial y^2}, \tag{18}$$

Physical conditions according to the current discussed problem are

$$\begin{aligned} &v_*(y,0)=0, v_*(0,t)=0, v_*(\infty,t)=0,\\ &T_*(y,0)=T_{*\infty}, T_*(0,t)=T_{*w}, T_*(k,t)=T_{*\infty},\\ &C_*(y,0)=C_{*\infty}, C_*(0,t)=C_{*w}, C_*(k,t)=C_{*\infty}.\end{aligned} \tag{19}$$

In the system of PDEs (16) - (19) v_* velocity component of OBNF along x-axis, T_* is fluid temperature, $T_{*\infty}$ is ambient temperature and T_{*w} is the wall temperature. C_* is fluid concentration, $C_{*\infty}$ is ambient concentration and C_{*w} is the wall concentration. λ is relaxation time, “its the time required to a fluid to return its initial equilibrium state after deformation.” λ_{*r} is retardation time, it can be defined as “The time that is actually required for the strain to reach its maximum value under a state of constant stress.”

Introducing some non dimensional quantities,

$$\varpi = \frac{v_*}{v_\bullet}, \xi = \frac{y}{k}, \mathfrak{I} = \frac{tv_\bullet}{k}, T = \frac{T_* - T_{*\infty}}{T_{*w} - T_{*\infty}}, C = \frac{C_* - C_{*\infty}}{C_{*w} - C_{*\infty}}, \tag{20}$$

since for Nanofluid some physical quantities are defined as [44],

$$\begin{aligned} &\rho_{nf} = \rho_f(1-\varphi)+\varphi\rho_s,\\ &(\rho\beta_T)_{nf} = (\rho\beta_T)_f(1-\varphi)+\varphi(\rho\beta_T)_s,\\ &(\rho\beta_C)_{nf} = \varphi(\rho\beta_C)_s+(\rho\beta_C)_f(1-\varphi),\\ &(\rho c_p)_{nf} = (1-\varphi)(\rho c_p)_f+\varphi(\rho c_p)_s,\\ &D_{nf} = D_f(1-\varphi),\\ &k_{nf} = k_f\left[\frac{k_s+2k_f-2\varphi(k_f-k_s)}{k_s+2k_f+\varphi(k_f-k_s)}\right],\\ &\mu_{nf} = \mu_f(1-\varphi)^{-2.5},\end{aligned} \tag{21}$$

now using the equations (20), (21) equations (16) - (19) reduced to following dimensionless form,

$$A_2\left(1+\lambda\frac{\partial}{\partial\mathfrak{I}}\right)\frac{\partial\varpi(\xi,\mathfrak{I})}{\partial\mathfrak{I}} = \left(1+\lambda_r\frac{\partial}{\partial\mathfrak{I}}\right)\frac{\partial^2\varpi(\xi,\mathfrak{I})}{\partial\xi^2} + A\left(1+\lambda\frac{\partial}{\partial\mathfrak{I}}\right)T(\xi,\mathfrak{I}) + A_1\left(1+\lambda\frac{\partial}{\partial\mathfrak{I}}\right)C(\xi,\mathfrak{I}), \tag{22}$$

$$\frac{\partial T(\xi,\mathfrak{I})}{\partial\mathfrak{I}} = \frac{1}{A_3}\frac{\partial^2 T(\xi,\mathfrak{I})}{\partial\xi^2}, \tag{23}$$

$$\frac{\partial C(\xi,\mathfrak{I})}{\partial\mathfrak{I}} = \frac{1}{A_4}\frac{\partial^2 C(\xi,\mathfrak{I})}{\partial\xi^2}, \tag{24}$$

$$\begin{aligned} &\varpi(\xi,0)=0, T(\mathfrak{I},0)=0, C(\xi,0)=0,\\ &\varpi(0,\mathfrak{I})=0, T(0,\mathfrak{I})=1, C(0,\mathfrak{I})=0,\\ &\varpi(\infty,\mathfrak{I})=0, T(1,\mathfrak{I})=0, C(1,\mathfrak{I})=0,\\ &\frac{\partial\varpi(\xi,\mathfrak{I})}{\partial\mathfrak{I}}|_{\mathfrak{I}=0},\end{aligned} \tag{25}$$

where,

$$\lambda = \frac{\lambda_* v_\bullet}{k}, \lambda_r = \frac{\lambda_{*r} v_\bullet}{k}, A_2 = \ell\ell_3 Re,\ A = Gr\ell_1\ell_3,\ A_1 = Gm\ell_2\ell_3,$$

$$\ell = (1-\varphi)+\varphi\frac{\rho_s}{\rho_f}, \ell_1 = (1-\varphi)+\varphi\frac{(\rho\beta_T)_s}{(\rho\beta_T)_f}, \ell_2 = \frac{(1-\varphi)+\varphi(\rho\beta_c)_s}{(\rho\beta_c)_f},$$

$$\ell_3 = \frac{1}{(1-\varphi)^{2.5}}, Re = \frac{v_\bullet k}{v}, Gr = \frac{g\beta_T\rho k^2(T_w - T_k)}{v_\bullet\mu},$$

$$Gm = \frac{g\beta_C\rho k^2(C_w - C_k)}{v_\bullet\mu},$$

$$A_3 = \frac{Pr\, Re\phi_2}{\phi_1}, A_4 = \frac{ScRe}{1-\phi}, Pr = \frac{\mu C_p}{k}, Sc = \frac{v_f}{D_f},$$

$$\phi_1 = \frac{k_s(1+2\phi)+k_f(2-2\phi)}{k_s(1-\phi)+k_f(\phi+2)}, \phi_2 = 1-\phi+\frac{(\rho c_p)_s}{(\rho c_p)_f}.$$

2.2. Exact solution

2.2.1. Temperature

Apply Caputo Fabrizio (CF) time fractional derivative Eq (2) on Eq (23), temperature equation with fractional derivative is as follows

$$^{CF}D^{\alpha}_{\mathfrak{I}}T(\xi,\mathfrak{I}) = \frac{1}{A_3}\frac{\partial^2 T(\xi,\mathfrak{I})}{\partial\xi^2}, \tag{26}$$

where, $^{CF}D^{\alpha}_{\mathfrak{I}}$ is Caputo Fabrizio fractional differential operator, α fractional parameter.

Apply Laplace transformation on Eq (26)

$$\frac{sa}{s+a_1}\overline{T}(\xi,s) = \frac{1}{A_3}\frac{\partial^2\overline{T}(\xi,s)}{\partial\xi^2}, \tag{27}$$

Laplace transform of $T(\xi,\mathfrak{I})$, is $\overline{T}(\xi,s)$.

Apply finite Fourier sine transformation on Eq (27)

$$\overline{T}_f(n,s) = \left(\frac{n\pi}{a_\circ A_3 + n\pi}\right)\left(\frac{a_1}{a_2 s} - \frac{a_1 - a_2}{a_2(s+a_2)}\right), \tag{28}$$

where, $\overline{T}_f(n,s)$ is fourier sine transform of $\overline{T}(\xi,s)$ and

$$a_2 = \frac{a_1(n\pi)^2}{aA_3 + n\pi},$$

now apply inverse laplace transformation

$$T_f(n,\mathfrak{I}) = \frac{1-(-1)^n}{n\pi} - \frac{(-1)^{n+1}}{n\pi} - a_3\exp(-a_2\mathfrak{I}), \tag{29}$$

$$a_3 = \left(\frac{n\pi}{a_\circ A_3 + n\pi}\right)\left(\frac{a_1 - a_2}{a_2}\right).$$

Finally use finite Fourier sine inverse transformation, the temperature is as follows

$$T(\xi,\mathfrak{T}) = 1-\xi-2\sum_{n=1}^{\infty} a_3\exp(-a_2\mathfrak{T})\sin(n\pi\xi). \tag{30}$$

2.2.2. Contraction

Apply Caputo Fabrizio (CF) time fractional derivative Eq (2) on Eq (24), contraction equation with fractional derivative is as bellow,

$$^{CF}D^{\alpha}_{\mathfrak{T}}C(\xi,s) = \frac{1}{\mathrm{A}_4}\frac{\partial^2 C(\xi,s)}{\partial\xi^2}. \tag{31}$$

Apply Laplace transformation on Eq (31)

$$\frac{sa}{s+a_1}\overline{C}(\xi,s) = \frac{1}{\mathrm{A}_4}\frac{\partial^2\overline{C}(\xi,s)}{\partial\xi^2}. \tag{32}$$

Apply finite Fourier sine transformation on Eq (32)

$$\overline{C}_f(n,s) = \left(\frac{n\pi}{a_\circ\mathrm{A}_4+n\pi}\right)\left(\frac{a_1}{a_5 s}-\frac{a_1-a_5}{a_2(s+a_5)}\right), \tag{33}$$

where,

$$a_5 = \frac{a_1(n\pi)^2}{a\mathrm{A}_4+n\pi}.$$

Now apply inverse laplace transformation

$$C_f(n,\mathfrak{T}) = \frac{1-(-1)^n}{n\pi}-\frac{(-1)^{n+1}}{n\pi}-a_4\exp(-a_2\mathfrak{T}), \tag{34}$$

$$a_4 = \left(\frac{n\pi}{a_\circ\mathrm{A}_4+n\pi}\right)\left(\frac{a_1-a_5}{a_5}\right).$$

Finally apply inverse finite Fourier sine transformation

$$C(\xi,\mathfrak{T}) = 1-\xi-2\sum_{n=1}^{\infty} a_4\exp(-a_5\mathfrak{T})\sin(n\pi\xi). \tag{35}$$

2.2.3. Velocity

Apply Caputo Fabrizio (CF) time fractional derivative Eq (2) on Eq (22), and get fractional velocity equation for FOBNF as follows,

$$\begin{aligned}\mathrm{A}_2\left(1+\lambda^{CF}D^{\alpha}_{\mathfrak{T}}\right)^{CF}D^{\alpha}_{\mathfrak{T}}\varpi(\xi,\mathfrak{T}) &= \left(1+\lambda_r{}^{CF}D^{\alpha}_{\mathfrak{T}}\right)\frac{\partial^2\varpi(\xi,\mathfrak{T})}{\partial\xi^2}\\ &+\mathrm{A}\left(1+\lambda^{CF}D^{\alpha}_{\mathfrak{T}}\right)T(\xi,\mathfrak{T})\\ &+\mathrm{A}_1\left(1+\lambda^{CF}D^{\alpha}_{\mathfrak{T}}\right)C(\xi,\mathfrak{T}).\end{aligned} \tag{36}$$

Taking the Laplace transformation to Eqs (36), the transformed problem is:

$$\begin{aligned}\mathrm{A}_2\tfrac{sa(1+s\lambda)}{s+a_1}\overline{\varpi}(\xi,s) &= \left(1+\lambda_r\tfrac{sa}{s+a_1}\right)\tfrac{\partial^2\overline{\varpi}(\xi,s)}{\partial\xi^2}+\mathrm{A}\left(1+\lambda\tfrac{sa}{s+a_1}\right)\overline{T}(\xi,s)\\ &+\mathrm{A}_1\left(1+\lambda\tfrac{sa}{s+a_1}\right)\overline{C}(\xi,s).\end{aligned} \tag{37}$$

Now, apply finite fourier sine transform

$$\begin{aligned}\mathrm{A}_2\tfrac{sa(1+s\lambda)}{s+a_1}\overline{\varpi}_f(n,s) &= \left(1+\lambda_r\tfrac{sa}{s+a_1}\right)(-n\pi)^2\overline{\varpi}_f(\xi,s)\\ &+\mathrm{A}\left(1+\lambda\tfrac{sa}{s+a_1}\right)\overline{T}_f(\xi,s)\\ &+\mathrm{A}_1\left(1+\lambda\tfrac{sa}{s+a_1}\right)\overline{C}_f(\xi,s),\end{aligned} \tag{38}$$

rearrange above Eq (38)

$$\overline{\varpi}_f(n,s) = \left[\frac{s+a_1}{s^2\Lambda+\mathrm{A}_6+s\Lambda_r}\right]\left[\frac{s\Lambda_1+a_1}{s+a_1}\mathrm{A}\overline{T}_f(\xi,s)+\frac{s\Lambda_1+a_1}{s+a_1}\mathrm{A}_1\overline{C}_f(\xi,s)\right],$$

where,

$$\Lambda_r = a\mathrm{A}_2+(n\pi)^2\left[1+\lambda_r a\right], \mathrm{A}_6 = a_1(n\pi), \Lambda = \lambda a\mathrm{A}_2, \Lambda_1 = 1+a\lambda,$$

use Eq (28) and Eq (33) in above equation

$$\overline{\varpi}_f(n,s) = \left[\frac{1}{(s+L_1)(s+L_2)}\right]\left[\frac{(s+L_3)(s+a_1)}{s(s+a_2)}L_6+\frac{(s+L_3)(s+a_1)}{a(s+a_5)}L_7\right], \tag{39}$$

where,

$$L_1 = \frac{all_3\mathrm{Re}+(n\pi^2)(1+\lambda_r a)+\sqrt{\left(all_3\mathrm{Re}+n\pi\right)^2+(n\pi)^2\lambda_r\left(a\lambda_r+2\right)+n\pi\mathrm{Re}all_3\left(2a\lambda_r+4n\pi\lambda a_2\right)}}{2\lambda all_3\mathrm{Re}},$$

$$L_2 = \frac{all_3\mathrm{Re}+(n\pi^2)(1+\lambda_r a)-\sqrt{\left(all_3\mathrm{Re}+n\pi\right)^2+(n\pi)^2\lambda_r\left(a\lambda_r+2\right)+n\pi\mathrm{Re}all_3\left(2a\lambda_r+4n\pi\lambda a_2\right)}}{2\lambda all_3\mathrm{Re}},$$

$$L_3 = \frac{a_1}{1+a\lambda}, L_6 = \left(\frac{n\pi}{a_\circ\mathrm{A}_3+n\pi}\right)\left((1+a\lambda)Grl_1l_3\right),$$

$$L_7 = \left(\frac{n\pi}{a_\circ\mathrm{A}_4+n\pi}\right)\left((1+a\lambda)Gml_2l_3\right).$$

Rearrange Eq (39) as follows,

$$\begin{aligned}\overline{\varpi}_f(n,s) &= \tfrac{1}{s}\left(\tfrac{a_1L_3L_6}{a_2L_1L_2}\right)+\tfrac{1}{s}\left(\tfrac{a_1L_3L_7}{a_2L_1L_2}\right)+\tfrac{1}{s+a_2}\left(\tfrac{a_1L_3-a_1a_2-a_2L_3+a_2{}^2}{a_2(L_1-a_2)(-L_2+a_2)}L_6\right)\\ &+\tfrac{1}{s+L_1}\left(\tfrac{a_1L_1+L_1L_3-a_1L_3+L_1{}^2}{L_1(L_1-L_2)(L_1-a_2)}L_6\right)+\tfrac{1}{s+L_2}\left(\tfrac{-a_1L_2-L_2L_3+a_1L_3-L_2{}^2}{L_2(L_1-L_2)(L_2-a_2)}L_6\right)\\ &+\tfrac{1}{s+a_2}\left(\tfrac{a_1L_3-a_1a_2-a_2L_3+a_2{}^2}{a_2(L_1-a_2)(-L_2+a_2)}L_7\right)+\tfrac{1}{s+L_1}\left(\tfrac{a_1L_1+L_1L_3-a_1L_3+L_1{}^2}{L_1(L_1-L_2)(L_1-a_2)}L_7\right)\\ &+\tfrac{1}{s+L_2}\left(\tfrac{-a_1L_2-L_2L_3+a_1L_3-L_2{}^2}{L_2(L_1-L_2)(L_2-a_2)}L_7\right),\end{aligned} \tag{40}$$

apply inverse laplace transform to Eq (40)

$$\begin{aligned}\varpi_f(n,\mathfrak{T}) &= \left(\tfrac{a_1L_3(L_6+L_7)}{a_2L_1L_2}\right)+\left(\tfrac{a_1L_3-a_1a_2-a_2L_3+a_2{}^2}{a_2(L_1-a_2)(-L_2+a_2)}L_6\right)\mathrm{e}^{-a_2\mathfrak{T}}\\ &+\left(\tfrac{a_1L_1+L_1L_3-a_1L_3+L_1{}^2}{L_1(L_1-L_2)(L_1-a_2)}L_6\right)\mathrm{e}^{-L_1\mathfrak{T}}+\left(\tfrac{-a_1L_2-L_2L_3+a_1L_3-L_2{}^2}{L_2(L_1-L_2)(L_2-a_2)}L_6\right)\mathrm{e}^{-L_2\mathfrak{T}}\\ &+\left(\tfrac{a_1L_3-a_1a_2-a_2L_3+a_2{}^2}{a_2(L_1-a_2)(-L_2+a_2)}L_7\right)\mathrm{e}^{-a_2\mathfrak{T}}+\left(\tfrac{a_1L_1+L_1L_3-a_1L_3+L_1{}^2}{L_1(L_1-L_2)(L_1-a_2)}L_7\right)\mathrm{e}^{-L_1\mathfrak{T}}\\ &+\left(\tfrac{-a_1L_2-L_2L_3+a_1L_3-L_2{}^2}{L_2(L_1-L_2)(L_2-a_2)}L_7\right)\mathrm{e}^{-L_2\mathfrak{T}},\end{aligned}$$

apply inverse fourier sine transformation and get the final result for velocity field as follows,

$$\begin{aligned}\varpi(\xi,\mathfrak{T}) &= 2\sum_{n=1}^{\infty}\Bigg[\left(\tfrac{a_1L_3(L_6+L_7)}{a_2L_1L_2}\right)+\left(\tfrac{a_1L_3-a_1a_2-a_2L_3+a_2{}^2}{a_2(L_1-a_2)(-L_2+a_2)}L_6\right)\mathrm{e}^{-a_2\mathfrak{T}}\\ &+\left(\tfrac{a_1L_1+L_1L_3-a_1L_3+L_1{}^2}{L_1(L_1-L_2)(L_1-a_2)}L_6\right)\mathrm{e}^{-L_1\mathfrak{T}}+\left(\tfrac{-a_1L_2-L_2L_3+a_1L_3-L_2{}^2}{L_2(L_1-L_2)(L_2-a_2)}L_6\right)\mathrm{e}^{-L_2\mathfrak{T}}\\ &+\left(\tfrac{a_1L_3-a_1a_2-a_2L_3+a_2{}^2}{a_2(L_1-a_2)(-L_2+a_2)}L_7\right)\mathrm{e}^{-a_2\mathfrak{T}}+\left(\tfrac{a_1L_1+L_1L_3-a_1L_3+L_1{}^2}{L_1(L_1-L_2)(L_1-a_2)}L_7\right)\mathrm{e}^{-L_1\mathfrak{T}}\\ &+\left(\tfrac{-a_1L_2-L_2L_3+a_1L_3-L_2{}^2}{L_2(L_1-L_2)(L_2-a_2)}L_7\right)\mathrm{e}^{-L_2\mathfrak{T}}\Bigg]\sin(n\pi\xi).\end{aligned} \tag{41}$$

2.2.4. Nusselt number

Nusselt number build the connection between heat transfer through conduction and convection. Since the dimensional Nusselt number is [45],

$$Nu = -\frac{k_{nf}}{k_f}\left(\frac{k}{T_w-T_\infty}\right)\left.\frac{\partial T}{\partial y}\right|_{y=0},$$

using equation (30) for the studied problem the Nusselt number reduced to the form,

$$Nu = -\frac{k_{nf}}{k_f}\left.\frac{\partial T}{\partial\xi}\right|_{\xi=0}. \tag{42}$$

Table 1
Heat transfer grease-based MoS_2 of OBNF Eq (42).

A_3	0	0.01	0.02	0.03	0.04
Nu	162.42	169.78	177.40	185.30	193.47
Heat Transfer enhancement	...	4.31%	9.23%	14.08%	19.11%

2.2.5. Sherwood number (Sh)

It is a dimensionless number used in mass-transfer operation and represent the effectiveness mass convection at the surface. Since the dimensional form of the Sherwood number is [45],

$$Sh = -D_{nf}\left(\frac{k}{C_w - C_\infty}\right)\frac{\partial C}{\partial y}\bigg|_{y=0},$$

using equation (35) for the studied problem the Sherwood number is

$$Sh = -D_{nf}\frac{C(\xi,\mathfrak{F})}{\partial \xi}\bigg|_{\xi=0}. \tag{43}$$

2.2.6. Skin friction

In fluid dynamics skin friction is also termed as shear stress. It is actually the force that is exerted by flowing liquid on solid surface. Nonzero shear stress in dimensional form for OBNF,

$$\left(1+\lambda\frac{\partial}{\partial t}\right)sf = \mu\left(1+\lambda_r\frac{\partial}{\partial t}\right)\frac{\partial \varpi}{\partial y},$$

after rearranging

$$sf = \mu_{nf}\frac{\left(1+\lambda_r\frac{\partial}{\partial t}\right)}{\left(1+\lambda\frac{\partial}{\partial t}\right)}\frac{\partial \varpi}{\partial y}, \tag{44}$$

using equation (21) the dimensionless skin friction for the studied problem is

$$sf = \frac{1}{(1-\phi)^{2.5}}\frac{\left(1+\lambda_r\frac{\partial}{\partial \mathfrak{F}}\right)}{\left(1+\lambda\frac{\partial}{\partial \mathfrak{F}}\right)}\frac{\partial \varpi}{\partial \xi}.$$

Now, as the fluid flow is between two vertical plates, the skin friction on each plate is calculated separately as follows,

$$sf_{lp} = \frac{1}{(1-\phi)^{2.5}}\frac{\left(1+\lambda_r\frac{\partial}{\partial \mathfrak{F}}\right)}{\left(1+\lambda\frac{\partial}{\partial \mathfrak{F}}\right)}\frac{\partial \varpi}{\partial \xi}\bigg|_{\xi=0}.$$

$$sf_{rp} = \frac{1}{(1-\phi)^{2.5}}\frac{\left(1+\lambda_r\frac{\partial}{\partial \mathfrak{F}}\right)}{\left(1+\lambda\frac{\partial}{\partial \mathfrak{F}}\right)}\frac{\partial \varpi}{\partial \xi}\bigg|_{\xi=1},$$

where, sf_{lp} is skin friction on the left plate and sf_{rp} on the right plate.

3. Validation of the numerical results

Fig. 2 is a comparison graph between Newtonian and non-Newtonian fluids. When $(\lambda_r)=0$ fluid reduced to Maxwell fluid [47] it flows faster than Oldroyd B fluid. Further when the both parameters λ and (λ_r) approaches to zero the fluid reduced to Newtonian fluid [46]. Clearly from the graph see that velocity of Newtonian fluid is greater than other two fluids. Which validated the study as Newtonian fluids flow faster as compare to the non-Newtonian fluids.

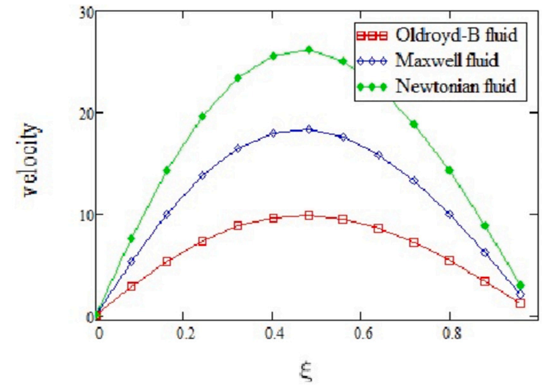

Fig. 2. Comparison between Newtonian fluid [46], Maxwell fluid [47] and Oldroyd-B nanofluid (OBNF).

Table 2
Mass transfer of grease-based MoS_2 of OBNF Eq (43).

A_4	0	0.01	0.02	0.03	0.04
Sh	0.69	0.70	0.70	0.70	0.71
Decrease in mass distribution	...	0.59%	1.21%	1.84%	2.51%

4. Result and discussions

This section includes all the discussion about the work on the open channel flow of a viscoelastic OBNF. First of all nondimensional approach is used to get dimensionless partial differential equation then use CF time-fractional derivative for fractional Oldroyd-B Nanofluid (FOBNF) just because fractional model has more important and many applications as compare to ordinary model of fluid. Laplace and finite fourier transformation techniques are jointly used for calculating exact mathematical solutions.

Table 1 represents the Nusselt number, against the different values of the coefficient A_3, and check the heat enhancement percentage, the heat transfer rate increases to 12.38%, by adding up to 4% nanoparticles. Table 2 represents the Sherwood number, for different values of A_4, and observe the percentage of decrease in mass transfer, the mass distribution decreases 2.14%, by adding up to 4% nanoparticles. Table 3 is for different values of skin friction from the lower plate to the upper plate, between the plates there is a unit difference therefore the share stress is calculated from zero to one, skin friction near the origin at the left plate is greater, as move towards the right plate away from origin the friction is decreased gradually.

Different physical quantities impact is observed with the help of graphical visualization of temperature and concentration distribution and velocity field. Physical quantities's (say Re, Pr, α, t, Sc, λ, λ_r, and Gm) influence is graphically demonstrated in Figs. 2-3. Some quantities support the fluid and enhance its flow and some minimize the transport ratio. The temperature $T(\xi,\mathfrak{F})$ profile for impact of different physical parameters represented in Figs. 3-6. Figs. 7-9 represent the impact of physical parameters on concentration $C(\xi,\mathfrak{F})$. Figs. 10-16 are graphical representation for velocity $\varpi(\xi,\mathfrak{F})$ under the impact of different parameters. Finally the Fig. 2 is for the comparison between the current studied fluid and Newtonian fluid.

4.1. Effect of temperature fluctuation with different parameter

4.1.1. Effect of temperature fluctuation with respect to Reynolds number Re

Fig. 3 is for the impact of dimensionless number Re on temperature $T(\xi,\mathfrak{F})$ distribution. Actually Reynolds number is the ratio between inertial and viscous forces. As the Re inversely proportional to temperature $T(\xi,\mathfrak{F})$. Temperature $T(\xi,\mathfrak{F})$ has maximum value at $Re=1$.

Table 3
Skin friction of grease based MoS_2 of OBNF from left plate to right plate Eq (44).

ξ	0	0.1	0.2	0.3	0.4	0.5	0.6	0.7	0.8	0.9	1
s_f	1.11	1.11	1.10	1.08	1.07	1.05	1.03	1.01	1.00	0.99	0.98

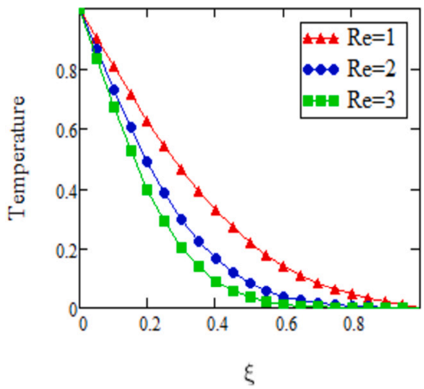

Fig. 3. The effect Re on $T(\xi, \mathfrak{T})$ of Oldroyd-B nanofluid (OBNF).

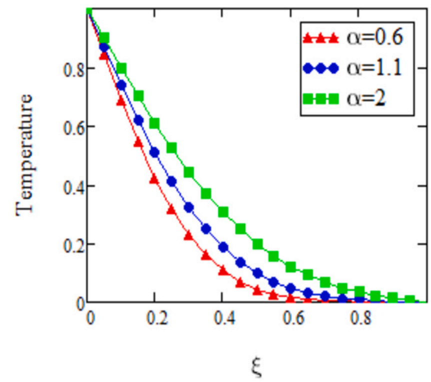

Fig. 5. The effect of α on $T(\xi, \mathfrak{T})$ of Oldroyd-B nanofluid (OBNF).

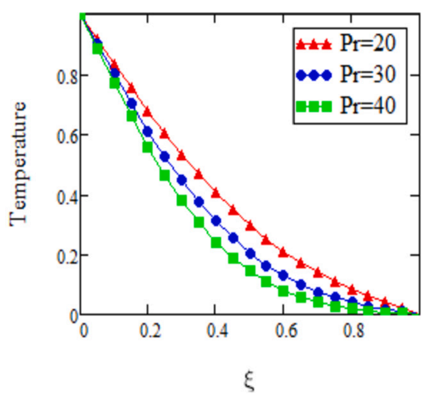

Fig. 4. The effect of Pr on $T(\xi, \mathfrak{T})$ of Oldroyd-B nanofluid (OBNF).

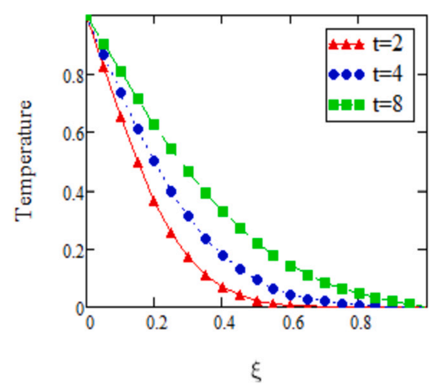

Fig. 6. The effect of time t on $T(\xi, \mathfrak{T})$ of Oldroyd-B nanofluid (OBNF).

4.1.2. Effect of temperature fluctuation with respect to Prandtl number Pr

Fig. 4 is for the impact of dimensionless number Prandtl number on temperature $T(\xi, \mathfrak{T})$ distribution, from figure see that the value of Pr increases $T(\xi, \mathfrak{T})$ decreases. When Pr increase, thickness of thermal boundary layer reduces. Since, the ratio between momentum and thermal diffusivity is called the Pr. Pr controls the relative thickening of thermal boundary layers and the momentum.

4.1.3. Effect of temperature fluctuation with respect to fractional parameter α

Fig. 5 is for the impact of α on $T(\xi, \mathfrak{T})$. The main advantage of using the fractional model is that more than one fluid layer for the investigation of fluid behavior and it provides more options for comparing the research to the other fractional model, which is impossible by a classical mathematical model. Clearly, see that as the value of α increases temperature $T(\xi, \mathfrak{T})$ is also increases therefore temperature $T(\xi, \mathfrak{T})$ of the fluid is directly proportional to α. The behavior of temperature reduced to classical model by taking $\alpha = 1$. Compared to the classical Oldroyd-B nanofluid model, the fractional-order Oldroyd-B nanofluid model provides a better explanation of heat transfer by varying degrees.

4.1.4. Effect of temperature fluctuation with respect to time

Fig. 6 is for the effect of time on $T(\xi, \mathfrak{T})$. The value of the temperature $T(\xi, \mathfrak{T})$ distribution decreases as the value of t is increased. Clearly, we see that viscous forces decrease when $T(\xi, \mathfrak{T})$ is increased. So, after pass age of time temperature of nanofluid is going to decrease.

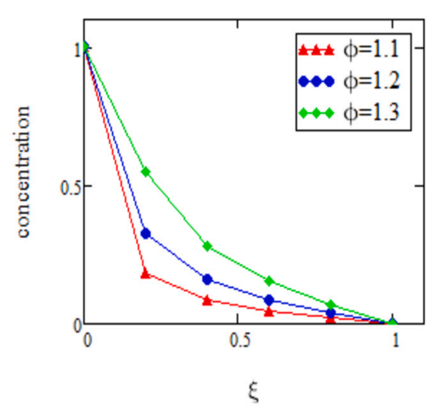

Fig. 7. The effect of $A_4 = \phi$ on $C(\xi, \mathfrak{T})$ of Oldroyd-B nanofluid (OBNF).

4.2. Effect of concentration fluctuation with dimensionless parameter

4.2.1. Effect of concentration fluctuation with respect to $\phi = A_4$

In Fig. 7 different values of $\phi = A_4$ against concentration $C(\xi, \mathfrak{T})$ distribution are discussed. The value of the concentration $C(\xi, \mathfrak{T})$ distribution decreases as the value of ϕ is increased. This is just because the reason that viscous forces rise, when the concentration distribution reduced.

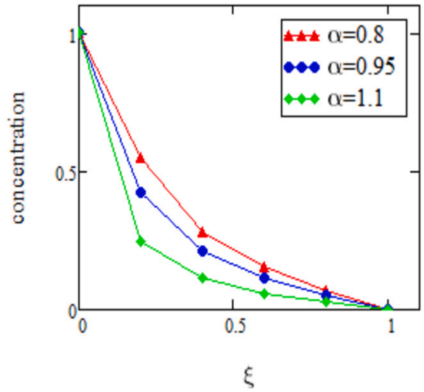

Fig. 8. The effect of α on $C(\xi,\mathfrak{I})$ of Oldroyd-B nanofluid (OBNF).

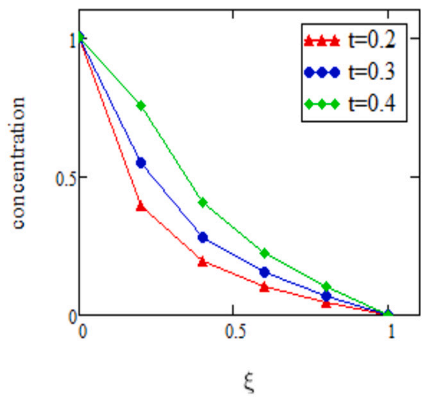

Fig. 9. The effect of time t on $C(\xi,\mathfrak{I})$ of Oldroyd-B nanofluid (OBNF).

4.2.2. Effect of concentration fluctuation with respect α

Fig. 8 is for the effect of α on concentration $C(\xi,\mathfrak{I})$ distribution. The behavior of α is same on contraction as on temperature $T(\xi,\mathfrak{I})$. Already discussed in Fig. 4.

4.2.3. Effect of concentration fluctuation with respect to time

Fig. 9 is for time effect on concentration $C(\xi,\mathfrak{I})$. The behavior of t is same on contraction as on temperature $T(\xi,\mathfrak{I})$. Already discussed in Fig. 6.

4.3. Effect of velocity fluctuation with dimensionless parameter

4.3.1. Effect of velocity fluctuation with respect to Schmidt number Sc

Fig. 10 shows Schmidt number Sc influence on the OBNF. Since ratio between mass diffusion and viscous forces is known as Schmidt number Sc, by increase in Sc increasing viscous forces and decreasing the mass diffusion, by which $\varpi(\xi,\mathfrak{I})$ decreases. In mass transfer Schmidt number Sc is equivalent of Prandtl Number Pr.

4.3.2. Effect of velocity fluctuation with respect to time

Fig. 11 is to investigate effect of time on velocity $\varpi(\xi,\mathfrak{I})$. Time is inversely proportional to the velocity $\varpi(\xi,\mathfrak{I})$ field of OBNF.

4.3.3. Effect of velocity fluctuation with respect to α

Fig. 12 is for the response of α. The basic benefit to study the fractional parameter is that it provides more than one layers to study the fluid behavior as compare to classical model. When $\alpha \to 0$ the fractional model reduced towards classical model. In the way researchers can compare their study with other fractional type fluids and classical fluid models.

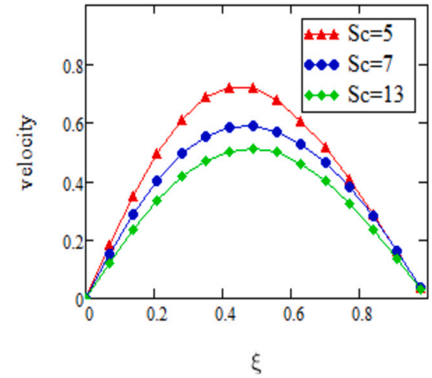

Fig. 10. The effect of Sc on $\varpi(\xi,\mathfrak{I})$ of Oldroyd-B nanofluid (OBNF).

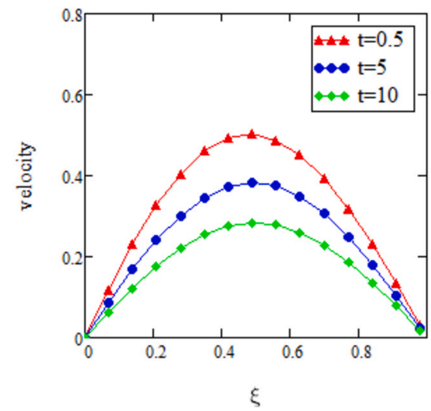

Fig. 11. The effect of t on $\varpi(\xi,\mathfrak{I})$ of Oldroyd-B nanofluid (OBNF).

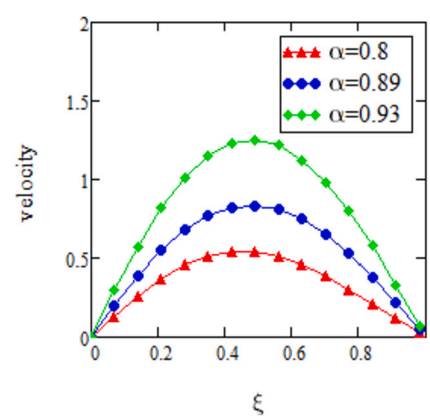

Fig. 12. The effect of α on $\varpi(\xi,\mathfrak{I})$ of Oldroyd-B nanofluid (OBNF).

4.3.4. Effect of velocity fluctuation with respect to retardation time λ_r

Fig. 13 plotted to investigate the behavior of retardation time λ_r on velocity $\varpi(\xi,\mathfrak{I})$ field. The retardation time is actually the time that required for the strain to reach its maximum value under a state of constant stress. Clearly, we can see that this material parameter is inversely proportional to the velocity $\varpi(\xi,\mathfrak{I})$ field. Hence, by increasing λ_r, the viscous forces decrease, which increases the fluid motion.

4.3.5. Effect of velocity fluctuation with respect to relaxation time λ

Fig. 14 is against the behavior of material parameter relaxation time λ of the fluid velocity $\varpi(\xi,\mathfrak{I})$ of OBNF. Relaxation time is actually the time that required to the system to its equilibrium state. When the values of relaxation time λ increase viscous forces are also increased and fluid motion is decreased.

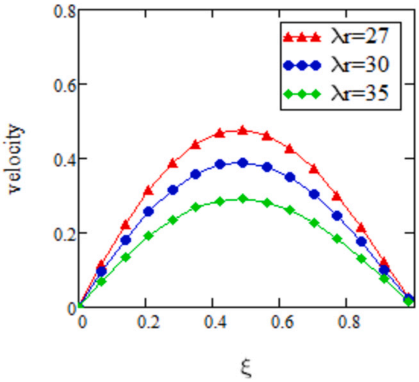

Fig. 13. The effect of λ_r on $\varpi(\xi,\mathfrak{I})$ of Oldroyd-B nanofluid (OBNF).

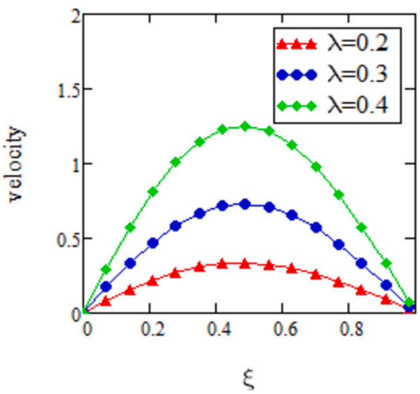

Fig. 14. The effect of λ on $\varpi(\xi,\mathfrak{I})$ of Oldroyd-B nanofluid (OBNF).

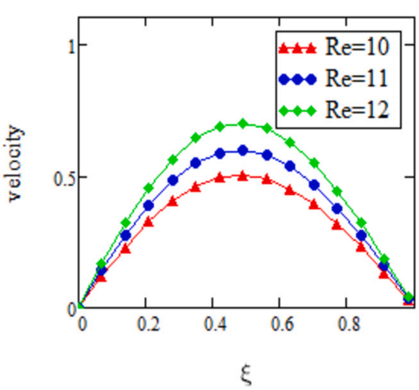

Fig. 15. The effect of Re on $\varpi(\xi,\mathfrak{I})$ of Oldroyd-B nanofluid (OBNF).

4.3.6. Effect of velocity fluctuation with respect to Reynolds number Re

Fig. 15 is for Reynolds number Re effect on velocity $\varpi(\xi,\mathfrak{I})$ profile. For greater Re the velocity $\varpi(\xi,\mathfrak{I})$ profile decreases. By definition, Re is actually a ratio between inertial and viscous forces. Re is directly proportional to the viscous forces. As the value of Re increases the viscous forces in the fluid enhance as a result the momentum boundary become thick and slow down the fluid.

4.3.7. Effect of velocity fluctuation with respect to Gm

Fig. 16 is for Gm effect on the velocity $\varpi(\xi,\mathfrak{I})$ field. Velocity $\varpi(\xi,\mathfrak{I})$ profile is directly proportional to Gm. Since, fluid moves from higher to low concentration area. See in the figure that when we increase the Gm the concentration level near the plate increase. This trend in the velocity field is physically true because when the value of Gm increases the concentration level near the plate increase and we know that fluid moves from higher concentration area to lower concentration area, therefore increasing trend has been observed.

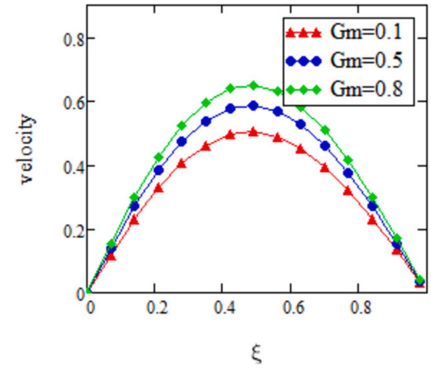

Fig. 16. The effect of Gm on $\varpi(\xi,\mathfrak{I})$ of Oldroyd-B nanofluid (OBNF).

5. Conclusion

In this paper, non-Newtonian nanofluid (OBNF) are studied in open channel flow along with heat and mass transfer. Meanwhile, several dimensionless numbers and skin friction are calculated and a comparison is performed between Newtonian and non-Newtonian fluids.

- It is found that the results are reducible to the classical Oldroyd-B nanofluid (OBNF) when α approaches to one while the velocity profile of Oldroyd-B nanofluid (OBNF) decrease by increasing the amount of molybdenum disulphide nanoparticles.
- It is identified that heat transfer rate is increased by using nanoparticles in the grease, which definitely will increase life time of different machineries and engines.
- The velocity of Oldroyd-B nanofluid (OBNF) is increased with respect to λ, Gm, and Gr, and decreased with respect to λ_r.
- Another aspect showed that the heat transfers rate increases up to 11.46% by increasing the value of A_4 and mass transfer rate reduces up to 2.51% of regular grease.

This work can be extended in different directions by considering different Newtonian and non-Newtonian fluid models. It can also be considered with different physical conditions and different directions such as spherical, cylindrical coordinates or flow over a thin needle, circular disk and stretching/shrinking sheet. The existing model can also be generalize by considering fractal-fractional differential operators of different kernels such as power decay, exponential or Mittage-Lefer kernel to find some hidden characteristics of the fluid flow. This model can also be considered for different base fluids in order to study various applications in science, engineering and renewable energy.

CRediT authorship contribution statement

Maria Javaid: Writing – review & editing, Writing – original draft, Investigation, Data curation, Conceptualization. **Junaid N. Chauhdary:** Writing – review & editing, Investigation, Formal analysis. **M. Yasar Javaid:** Resources, Methodology, Investigation. **Muhammad Farooq:** Writing – review & editing, Visualization, Validation, Supervision, Project administration, Conceptualization. **Faisal Saleem:** Formal analysis, Visualization, Writing – review & editing. **M. Imran:** Writing – review & editing, Visualization, Software. **Ijaz Hussain:** Visualization, Writing – review & editing, Investigation. **M. Sultan:** Writing – review & editing, Validation, Project administration. **M. Imran Khan:** Writing – review & editing, Visualization, Resources, Methodology. **Mohammad Ilyas Khan:** Writing – review & editing, Visualization, Validation, Methodology. **Mohammad Rehan:** Writing – review & editing, Resources, Funding acquisition. **Fahid Riaz:** Writing – review & editing, Resources, Funding acquisition, Formal analysis.

Declaration of competing interest

The authors declare that there is no conflict of interest.

Data availability

Data will be made available on request.

Acknowledgement

The authors extend their appreciation to the Deanship of Research and Graduate Studies at King Khalid University for funding this work through Large Research Project under grant number RGP2/533/45.

References

[1] S.U. Choi, J.A. Eastman, Enhancing thermal conductivity of fluids with nanoparticles (No. ANL/MSD/CP-84938; CONF-951135-29), Argonne National Lab. (ANL), Argonne, IL, United States, 1995.
[2] O.K. Koriko, N.A. Shah, S. Saleem, J.D. Chung, A.J. Omowaye, T. Oreyeni, Exploration of bioconvection flow of MHD thixotropic nanofluid past a vertical surface coexisting with both nanoparticles and gyrotactic microorganisms, Sci. Rep. 11 (1) (2021) 16627.
[3] F.U. Rehman, S. Nadeem, H.U. Rehman, R.U. Haq, Thermophysical analysis for three-dimensional MHD stagnation-point flow of nano-material influenced by an exponential stretching surface, Results Phys. 8 (2018) 316–323.
[4] M. Sheikholeslami, Magnetic field influence on nanofluid thermal radiation in a cavity with tilted elliptic inner cylinder, J. Mol. Liq. 229 (2017) 137–147.
[5] A.J. Chamkha, S. Abbasbandy, A.M. Rashad, K. Vajravelu, Radiation effects on mixed convection over a wedge embedded in a porous medium filled with a nanofluid, Transp. Porous Media 91 (2012) 261–279.
[6] X. Wang, Y. Song, C. Li, Y. Zhang, H.M. Ali, S. Sharma, Z. Zhou, Nanofluids application in machining: a comprehensive review, Int. J. Adv. Manuf. Technol. 131 (5) (2024) 3113–3164.
[7] Z. Liu, S. Li, T. Sadaf, S.U. Khan, F. Alzahrani, M.I. Khan, S.M. Eldin, Numerical bio-convective assessment for rate type nanofluid influenced by Nield thermal constraints and distinct slip features, Case Stud. Therm. Eng. 44 (2023) 102821.
[8] M.M. Bhatti, R. Ellahi, Numerical investigation of non-Darcian nanofluid flow across a stretchy elastic medium with velocity and thermal slips, Numer. Heat Transf., Part B, Fundam. 83 (5) (2023) 323–343.
[9] S. Dinarvand, M. Behrouz, S. Ahmadi, P. Ghasemi, S. Noeiaghdam, U. Fernandez-Gamiz, Mixed convection of thermomicropolar AgNPs-GrNPs nanofluid: an application of mass-based hybrid nanofluid model, Case Stud. Therm. Eng. 49 (2023) 103224.
[10] M. Abdul Basit, M. Imran, S.A. Khan, A. Alhushaybari, R. Sadat, M.R. Ali, Partial differential equations modeling of bio-convective sutterby nanofluid flow through paraboloid surface, Sci. Rep. 13 (1) (2023) 6152.
[11] M.J. Hasan, A.K. Azad, R. Hossain, M.M. Rahman, M.F. Karim, Analysis of mixed convection under radiation and magnetohydrodynamics utilizing kerosene-CNT nanofluid in a lid-driven cavity, Int. J. Thermofluids 21 (2024) 100528.
[12] R. Hossain, A.K. Azad, M.J. Hasan, M.M. Rahman, Radiation effect on unsteady MHD mixed convection of kerosene oil-based CNT nanofluid using finite element analysis, Alex. Eng. J. 61 (11) (2022) 8525–8543.
[13] Z. Islam, A.K. Azad, M.J. Hasan, R. Hossain, M.M. Rahman, Unsteady periodic natural convection in a triangular enclosure heated sinusoidally from the bottom using CNT-water nanofluid, Results Eng. 14 (2022) 100376.
[14] A.K. Azad, M.J. Hasan, M.F. Karim, E.M.M. Alam, M.M. Rahman, Rotational effect of a cylinder on hydro-thermal characteristics in a partially heated square enclosure using CNT-water nanofluid, Heliyon 9 (12) (2023).
[15] R. Hossain, M.J. Hasan, A.K. Azad, M.M. Rahman, Numerical study of low Reynolds number effect on MHD mixed convection using CNT-oil nanofluid with radiation, Results Eng. 14 (2022) 100446.
[16] R. Hossain, A.K. Azad, M.J. Hasan, M.M. Rahman, Thermophysical properties of kerosene oil-based CNT nanofluid on unsteady mixed convection with MHD and radiative heat flux, Int. J. Eng. Sci. Technol. 35 (2022) 101095.
[17] M.J. Hasan, A.K. Azad, Z. Islam, R. Hossain, M.M. Rahman, Periodic unsteady natural convection on CNT nano-powder liquid in a triangular shaped mechanical chamber, Int. J. Thermofluids 15 (2022) 100181.
[18] A.K. Azad, S. Parvin, M.M.K. Chowdhury, Effects of Hartmann number on combined convection in a channel with cavity using Cu-water nanofluid, in: AIP Conference Proceedings, vol. 1851, AIP Publishing, 2017, June.
[19] J. Shah, F. Ali, N. Khan, Z. Ahmad, S. Murtaza, I. Khan, O. Mahmoud, MHD flow of time-fractional Casson nanofluid using generalized Fourier and Fick's laws over an inclined channel with applications of gold nanoparticles, Sci. Rep. 12 (1) (2022) 17364.
[20] S. Murtaza, P. Kumam, A. Kaewkhao, N. Khan, Z. Ahmad, Fractal fractional analysis of non linear electro osmotic flow with cadmium telluride nanoparticles, Sci. Rep. 12 (1) (2022) 20226.
[21] Z. Ahmad, F. Ali, M.A. Almuqrin, S. Murtaza, F. Hasin, N. Khan, et al., Dynamics of love affair of Romeo and Juliet through modern mathematical tools: a critical analysis via fractal-fractional differential operator, Fractals 30 (05) (2022) 2240167.
[22] I. Podlubny, Fractional Differential Equations, Academic Press, San Diego, 1999.
[23] Y. Zhaosheng, L. Jianzhong, Numerical research on the coherent structure in the viscoelastic second-order mixing layers, Appl. Math. Mech. 19 (8) (1998) 717–723.
[24] R.G. Larson, The Structure and Rheology of Complex Fluids, Topics in Chemical Engineering, vol. 86, Oxford University Press, New York-Oxford, 1999, p. 108.
[25] T. Odzijewicz, A.B. Malinowska, D.F. Torres, Fractional variational calculus with classical and combined Caputo derivatives, Nonlinear Anal. 75 (3) (2012) 1507–1515.
[26] D. Vieru, C. Fetecau, N.A. Shah, S.J. Yook, Unsteady natural convection flow due to fractional thermal transport and symmetric heat source/sink, Alex. Eng. J. 64 (2023) 761–770.
[27] S. Abbas, M. Ahmad, M. Nazar, M. Amjad, H. Ali, A.Z. Jan, Heat and mass transfer through a vertical channel for the Brinkman fluid using Prabhakar fractional derivative, Appl. Therm. Eng. 232 (2023) 121065.
[28] I. Siddique, R. Adrees, H. Ahmad, S. Askar, MHD free convection flows of Jeffrey fluid with Prabhakar-like fractional model subject to generalized thermal transport, Sci. Rep. 13 (1) (2023) 9289.
[29] D. Vieru, C. Fetecau, General solutions for MHD motions of ordinary and fractional Maxwell fluids through porous medium when differential expressions of shear stress are prescribed on boundary, Mathematics 12 (2) (2024) 357.
[30] A.U. Rehman, C. Chunxia, M. Bilal Riaz, A. Atangana, S. Xiange, A comparative analysis of fractional model of second grade fluid subject to exponential heating: application of novel hybrid fractional derivative operator, Arab J. Basic Appl. Sci. 31 (1) (2024) 1–17.
[31] J. Beddrich, E. Suli, B. Wohlmuth, Numerical simulation of the time-fractional Fokker–Planck equation and applications to polymeric fluids, J. Comput. Phys. 497 (2024) 112598.
[32] M. Paszkowski, Assessment of the effect of temperature, shear rate and thickener content on the thixotropy of lithium lubricating greases, Proc. Inst. Mech. Eng., Part J J. Eng. Tribol. 227 (3) (2013) 209–219.
[33] M. Saeed, M.H. Kim, Heat transfer enhancement using nanofluids (Al2O3-H2O) in mini-channel heatsinks, Int. J. Heat Mass Transf. 120 (2018) 671–682.
[34] F. Schüler, M. Holynska, T. Henry, M. Buttery, K. Meier-Kirchner, C. Göhringer, Development of a space grease lubricant with long-term-storage properties, Lubricants 12 (3) (2024) 72.
[35] M. Paszkowski, Assessment of the effect of temperature, shear rate and thickener content on the thixotropy of lithium lubricating greases, Proc. Inst. Mech. Eng., Part J J. Eng. Tribol. 227 (3) (2013) 209–219.
[36] Y. Zhou, R. Bosman, P.M. Lugt, A master curve for the shear degradation of lubricating greases with a fibrous structure, Tribol. Trans. 62 (1) (2019) 78–87.
[37] X. Fan, Y. Xia, L. Wang, Tribological properties of conductive lubricating greases, Friction 2 (2014) 343–353.
[38] A. Atangana, Fractal-fractional differentiation and integration: connecting fractal calculus and fractional calculus to predict complex system, Chaos Solitons Fractals 102 (2017) 396–406.
[39] H.T. Qi, J.G. Liu, Some duct flows of a fractional Maxwell fluid, Eur. Phys. J. Spec. Top. 193 (2011) 71–79.
[40] D. Tripathi, Peristaltic transport of fractional Maxwell fluids in uniform tubes: applications in endoscopy, Comput. Math. Appl. 62 (3) (2011) 1116–1126.
[41] L. Debnath, D. Bhatta, Integral Transforms and Their Applications, second ed., Chapman and Hall/CRC Press, Boca Raton-London-New York, 2006.
[42] F. Salah, Z.A. Aziz, D.L.C. Ching, New exact solution for Rayleigh Stokes problem of Maxwell fluid in a porous medium and rotating frame, Results Phys. 1 (1) (2011) 9–12.
[43] A. Khalid, I. Khan, A. Khan, S. Shafie, Unsteady MHD free convection flow of Casson fluid past over an oscillating vertical plate embedded in a porous medium, Int. J. Eng. Sci. Technol. 18 (3) (2015) 309–317.
[44] N. Khan, Z. Ahmad, H. Ahmad, F. Tchier, X.Z. Zhang, S. Murtaza, Dynamics of chaotic system based on image encryption through fractal-fractional operator of non-local kernel, AIP Adv. 12 (5) (2022).
[45] N. Khan, F. Ali, M. Arif, Z. Ahmad, A. Aamina, I. Khan, Maxwell nanofluid flow over an infinite vertical plate with ramped and isothermal wall temperature and concentration, Math. Probl. Eng. 2021 (2021) 1–19.
[46] A. Khalid, I. Khan, S. Shafie, Exact solutions for free convection flow of nanofluids with ramped wall temperature, Eur. Phys. J. Plus 130 (2015) 1–14.
[47] N. Khan, F. Ali, Z. Ahmad, S. Murtaza, A.H. Ganie, I. Khan, S.M. Eldin, A time fractional model of a Maxwell nanofluid through a channel flow with applications in grease, Sci. Rep. 13 (1) (2023) 4428.